Electronic Supplementary Material (ESI) for Physical Chemistry Chemical Physics.
This journal is © the Owner Societies 2020

Supplementary Information: The carbon and oxygen K-edge NEXAFS spectra of CO^+

Rafael C. Couto,[*,†] Ludvig Kjellsson,[‡,¶] Hans Ågren,[*,‡,§,†] Vincenzo Carravetta,[‖] Stacey L. Sorensen,[⊥] Markus Kubin,[#] Christine Bülow,[#,@] Martin Timm,[#] Vicente Zamudio-Bayer,[#] Bernd von Issendorff,[@] J. Tobias Lau,[#,@] Johan Söderström,[‡] Jan-Erik Rubensson,[‡] and Rebecka Lindblad[⊥,#,△]

†*Department of Theoretical Chemistry and Biology, School of Chemistry, Biotechnology and Health, Royal Institute of Technology, SE-106 91 Stockholm, Sweden*

‡*Department of Physics and Astronomy, Uppsala University, Box 516, SE-751 20 Uppsala, Sweden*

¶*European XFEL GmbH, Holzkoppel 4, 22869 Schenefeld, Germany*

§*Tomsk State University, 36 Lenin Avenue, Tomsk, Russia*

‖*IPCF-CNR, via Moruzzi 1, 56124 Pisa, Italy*

⊥*Department of Physics, Lund University, Box 118, S-22100 Lund, Sweden*

#*Abteilung für Hochempfindliche Röntgenspektroskopie, Helmholtz-Zentrum Berlin für Materialien und Energie, Albert-Einstein-Str. 15, 12489 Berlin, Germany*

@*Physikalisches Institut, Albert-Ludwigs-Universität Freiburg, Hermann-Herder-Str. 3, 79104 Freiburg, Germany*

△*Inorganic Chemistry, Department of Chemistry - Ångström Laboratory, Uppsala University , SE-75121 Uppsala , Sweden*

E-mail: rcc@kth.se; hagren@kth.se

State-averaged natural orbitals

In Figs. S1 and S2 are presented the MS-RASPT2 state-averaged natural orbitals of CO^+ used in the calculation of the full spectrum presented in Figs. 1 and 5 of the main text and Figs. S3 (bottom panels), S4 (bottom panels), S5 to S9.

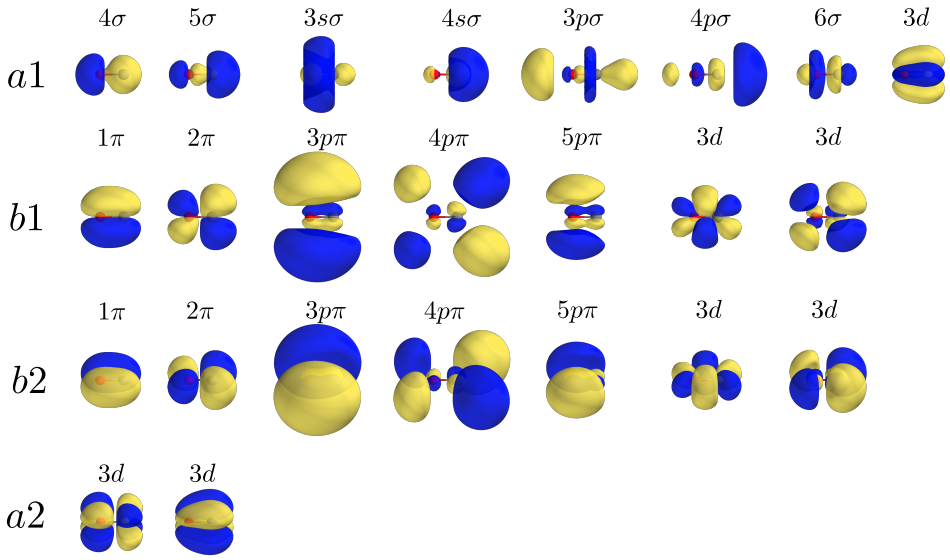

Figure S1: State-averaged natural molecular orbitals, for each irreducible representation in the C_{2v} Abelian point group, used in the MS-RASPT2 calculations of the full NEXAFS spectrum of CO^+ at the carbon K-edge.

Evaluation of RASSCF space

In order to compute the full spectrum, focusing on the high energy region of the NEXAFS spectrum, the RAS3 space was used, as described in the main text. The results presented in the main text are from calculations where we considered a maximum of three electrons in the RAS3 space. To evaluate this approximation, we computed the NEXAFS spectrum considering the same active space as described in the main text, but considering a maximum occupation of one, two and three electrons in the RAS3 space, which is presented in Fig. S3 for both carbon (left panels) and oxygen (right panels) K-edges. Through these results, it is clear that the increase in the number of electrons in the RAS3 space leads to a better agreement

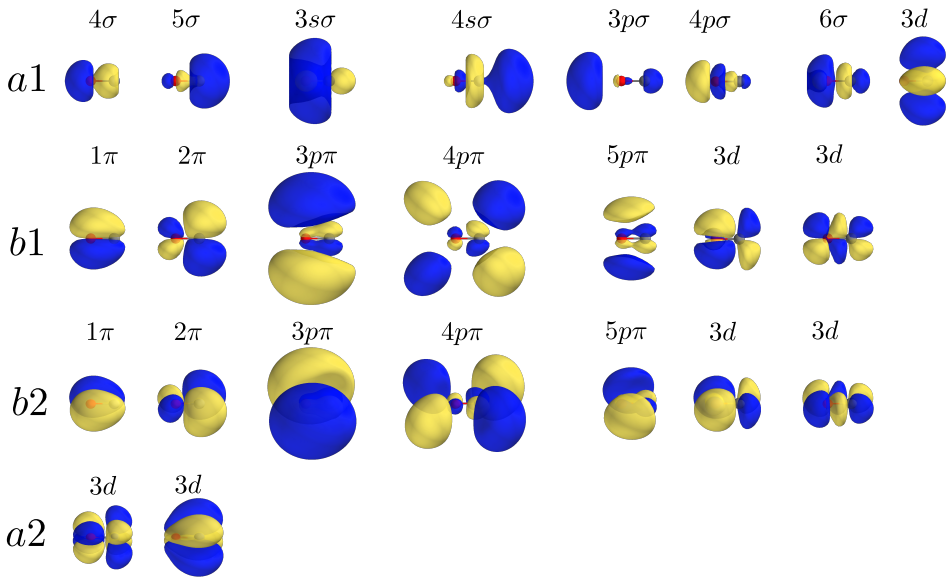

Figure S2: State-averaged natural molecular orbitals, for each irreducible representation in the C_{2v} Abelian point group, used in the MS-RASPT2 calculations of the full NEXAFS spectrum of CO^+ at the oxygen K-edge.

with the experimental features at the high energy region of the NEXAFS spectrum. This change affects the whole spectrum, not only the peak positions but also their intensities. In the case of the carbon edge (Fig. S3 left panels), when considering one electron in RAS3, not only the transitions are sparser, we see intensities in regions where nothing is seen in the experiment, like the peak at 293 eV. Moreover, when considering two electrons in RAS3, an overly intense peak appears at 307 eV. At the oxygen K-edge, the same problems are observed, with the best results coming from the consideration of three electrons in RAS3.

Another analysis that was made concerned the size of the RAS3 active space. As mentioned in the previous section, the use of the RAS3 space aimed at the assessment of the high energy part of the NEXAFS spectrum, which shows a high density of states. Due to this, a large active space was needed in order to get a good description of this region. The staring point was placing the 4σ, 5σ and the two 1π orbitals in the RAS2 space, which remains the same for all results presented in Fig. S4. For clarity, the RAS3 space was labeled according to the four irreducible representation in the C_{2v} Abelian point group, namely RAS3(a1,b1,b2,a2). The starting configuration was the RAS3(4,4,4,2) (bottom panels of

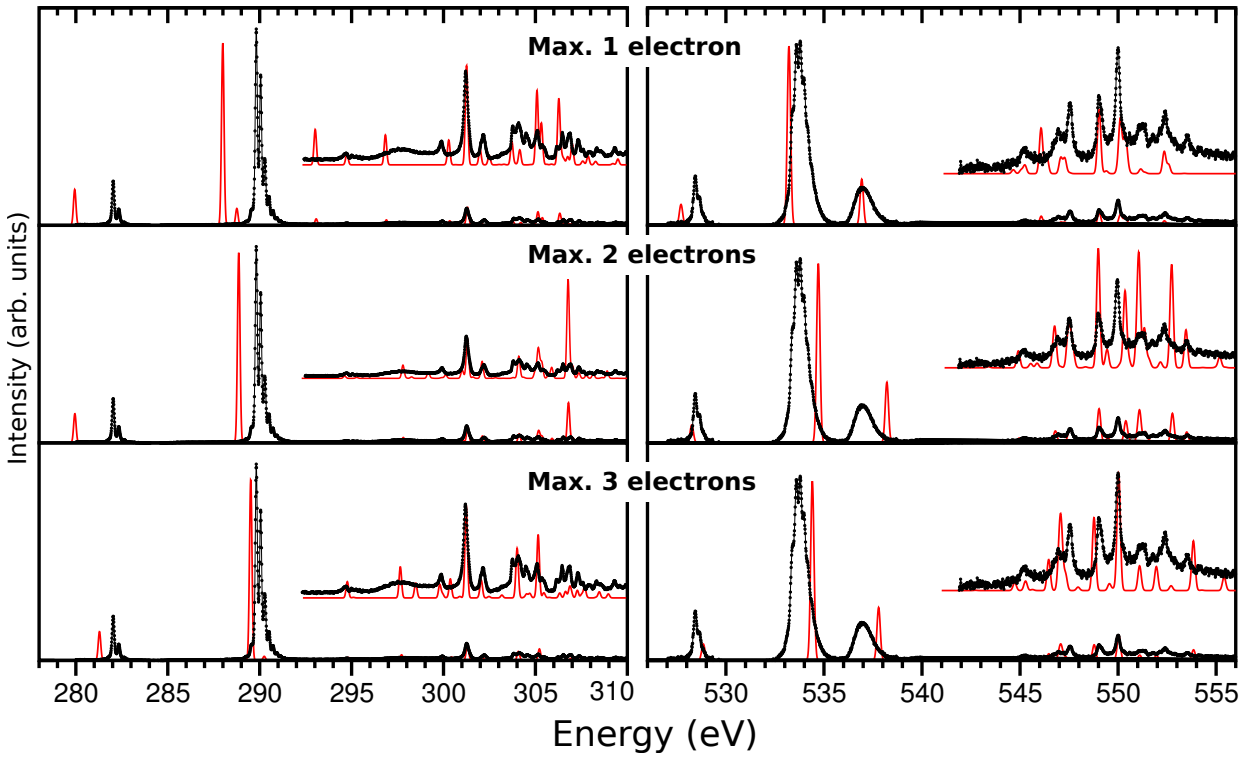

Figure S3: CO^+ NEXAFS spectrum at carbon (left panels) and oxygen (right panels) K-edge considering a maximum of one (top), two (middle) and three (bottom) electrons in the RAS3 space. The theoretical results (black) are compared with the experiment. In order to match most experimental features in the high energy region (between 294 and 310 eV) of carbon K-edge spectrum, the theoretical spectra were shifted by -1.02, -2.04 and -1.02 eV in the top, middle and bottom panels, respectively. At the oxygen K-edge high energy region (between 544 and 555 eV), the theoretical spectra were shifted by -0.7, -0.3 and -0.2 eV in the top, middle and bottom panels, respectively.

Fig. S4), which showed poor agreement at both carbon and oxygen K-edges. By increasing the number of orbitals in RAS3, we were able to approach good agreement with the experimental features. For the carbon K-edge (Fig. S4 left panels), the theoretical profile improves significantly after the inclusion of 6 orbitals in the a1 symmetry, showing a substantial reduction of the intensities above 305 eV. At the oxygen edge (Fig. S4 left panels) we observe major improvements from RAS3(6,5,5,2) and above, for which the important intense peak at 549 eV is observed. In both cases, the best results were obtained for RAS3(6,6,6,2). Attempts were made to increase the active space size, but the computational costs were too high.

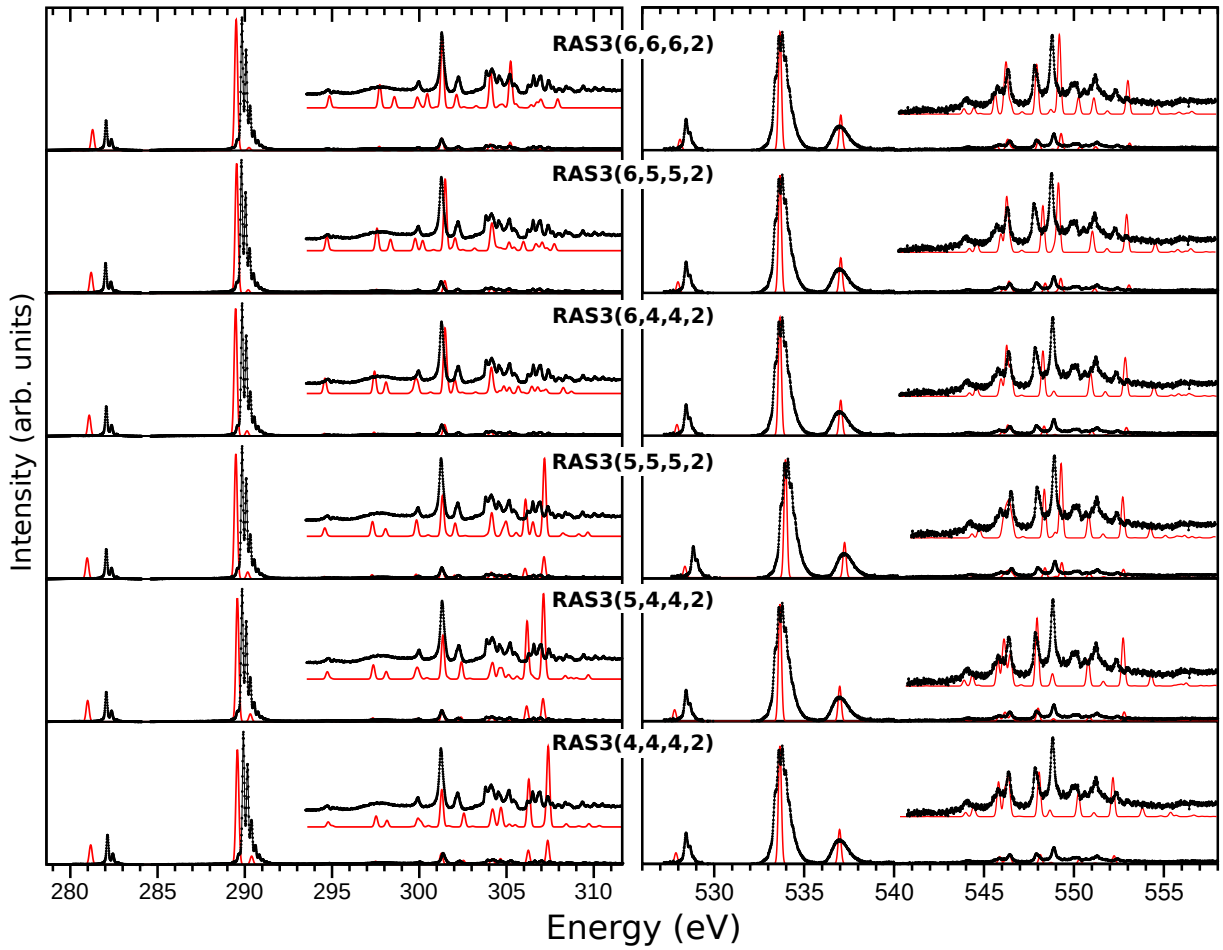

Figure S4: Theoretical (red curve) and experimental (black curve) CO^+ NEXAFS spectra at the carbon (left) and oxygen (right) K-edge considering different RAS3 space configurations. In all cases the ANO-RCC-VQZP basis set and auxiliary 8s6p4s Rydberg basis were used, and the RAS2 comprehended the 4σ, 5σ and the two 1π orbitals. The labels represent the number of orbitals in each irreducible symmetry following RAS3(a1,b1,b2,a2). All theoretical spectra were shifted in energy to match the RAS3(6,6,6,2) spectrum, which was shifted to match most experimental features.

Transition dipole moment gauge

As mentioned before, the transition dipole moments (TDM) used in the computations of the NEXAFS spectra were obtained in the velocity gauge. In Fig. S5, the NEXAFS spectra are shown considering length and velocity gauge TDMs and the difference between them, for both carbon and oxygen K-edges. As one can see, the 2π transition is the most affected, where the length gauge gives a smaller intensity, around 8% and 3% for carbon and oxygen K-

edges, respectively. At the high energy part, the difference between gauges are smaller, with bigger differences at the oxygen edge up to 1%. Due to this differences, the velocity gauge was used in all our simulations due to its better accuracy in the current implementation.[1]

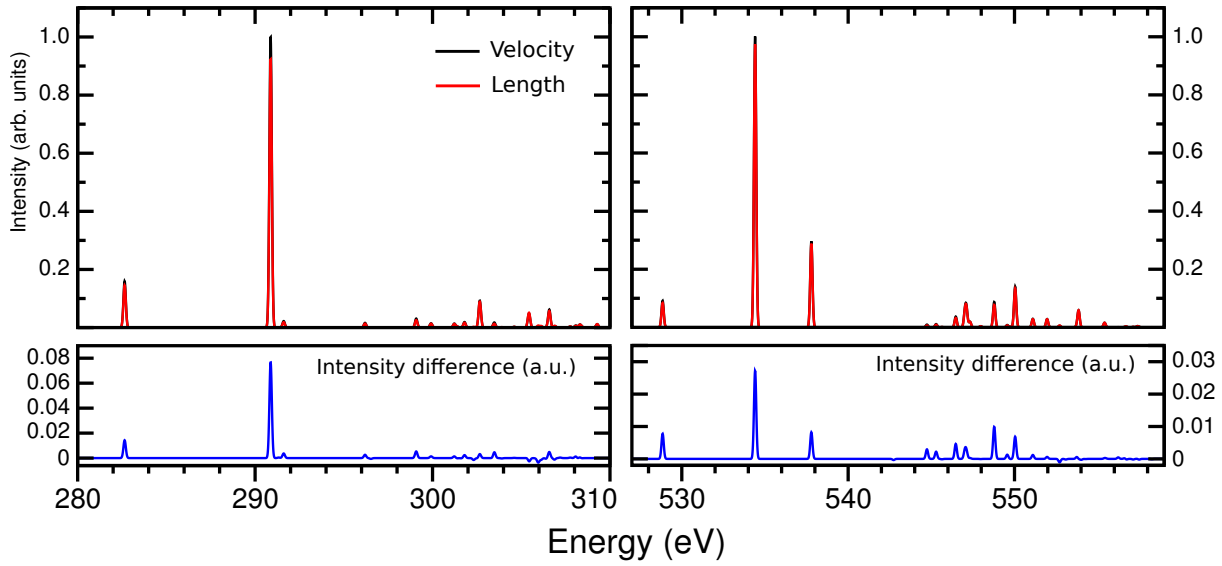

Figure S5: Theoretical NEXAFS spectra of CO^+ at the carbon (left) and oxygen (right) K-edges considering the length (red curve) and velocity (black curve) gauge of the transition dipole moments. The bottom panels show the difference between length and velocity gauges.

Spin-orbit coupling

In order to evaluate if the spin-orbit coupling would have any effect in the NEXAFS of CO^+, extra MS-RASPT2 calculations were performed for the quartet core-excited states. By considering the doublets and quartets states, a RASSI calculation was performed with the Spin-Orbit directive and the results are shown in Fig. S6 for both carbon and oxygen K-edges. As can be seen, the spin-orbit coupling shows no major effects in the final NEXAFS spectrum, with differences below 0.1% in both edges. Due to this, the spin-orbit coupling was neglected in the simulations presented here and in the main text.

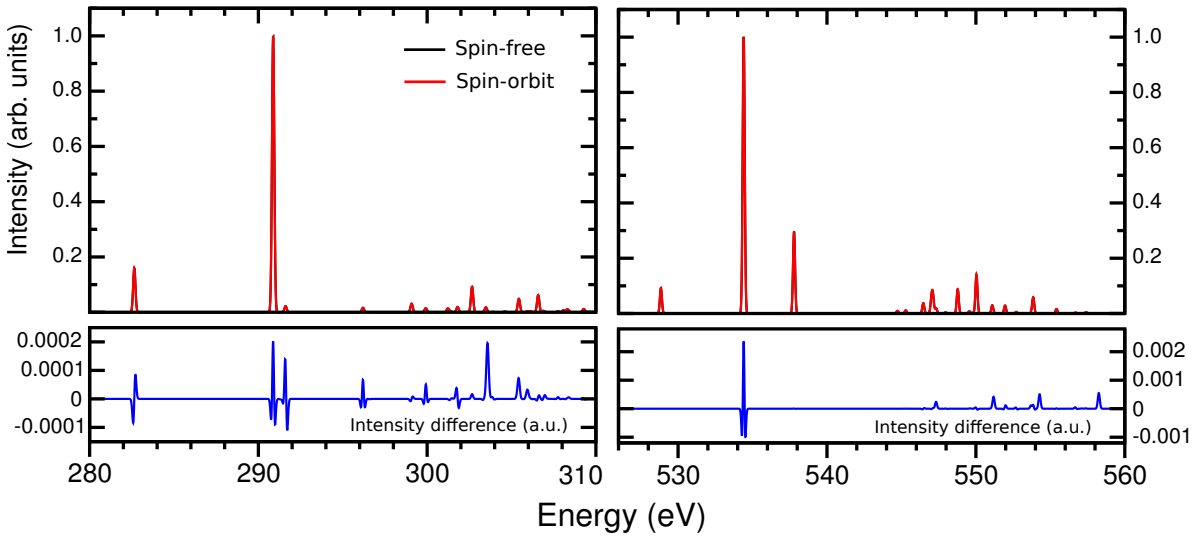

Figure S6: Theoretical NEXAFS spectra of CO^+ at the carbon (left) and oxygen (right) K-edges for spin-free (black curve) and spin-orbit coupling (red curve) calculations. The bottom panels shows the difference between spin-free and spin-orbit spectra.

Exchange integrals

Tab. S1 presents the computed exchange integrals mentioned in the main text in support of the explanation of the 2π splitting of NEXAFS spectra of CO^+. These results were obtained through a simple Hartree-Fock calculation using the equivalent core-hole approximation (Z+1), and the aug-cc-pVDZ basis set.

Table S1: Values for the exchange integrals related the $1s$, 5σ and 2π orbitals, for carbon (2σ) and oxygen (1σ) K-edges.

Term	x10^{-3} a.u.
$[2\sigma, 2\pi\|2\pi, 2\sigma]$	19.27
$[5\sigma, 2\pi\|2\pi, 5\sigma]^1$	41.29
$[1\sigma, 2\pi\|2\pi, 1\sigma]$	8.34
$[5\sigma, 2\pi\|2\pi, 5\sigma]^2$	82.11

[1]Carbon K-edge

[2]Oxygen K-edge

Experimental vibrational constants

The transitions to the two lowest lying states for both the carbon and oxygen K-edges are shown in Fig. S7 together with the curve fits in the Franck-Condon analysis. This analysis was used to extract the vibrational constants in Tab. 1 in the main manuscript. Only the vibrational ground state was included in the fits, and we note that a small peak at 289.55 eV at the low energy side of the carbon K-edge $2\sigma^{-1}5\sigma^{-1}2\pi$ resonance indicates a small amount of molecules in a vibrationally excited state. These are related to the Penning ionization process in the ion source.[2] At the oxygen K-edge this is not as pronounced, but visible as a shoulder at 533.1 eV. As described in the main manuscript, the high energy $2\sigma^{-1}5\sigma^{-1}2\pi$(H) state at the carbon K-edge is not observed experimentally. The corresponding state at the oxygen K-edge, $1\sigma^{-1}5\sigma^{-1}2\pi$(H), is clearly observed, but as it lacks clear vibrational structure, no Franck-Condon analysis is made. A comparison between our results and available literature is presented in Tab. S2.

Table S2: Vibrational constants for the C($1s^{-1}$) and O($1s^{-1}$) states of CO^+ obtained in our experimental analysis, and compared with the literature values taken from Matsumoto et al.[3]

State	T_e[eV]		ω_e[meV]		$\omega_e\chi_e$[meV]		ΔR_e[Å]	
	This work	Literature	This work	Literature	This work	Literature	This work	Literature
C $1s^{-1}$	282.00	-	310.9 ± 20	307.4	1.4 ± 1.1	2.9	-0.037	-0.0514
O $1s^{-1}$	528.48	-	225.3 ± 15	231.1	0.3 ± 0.15	0.87	0.047	0.037

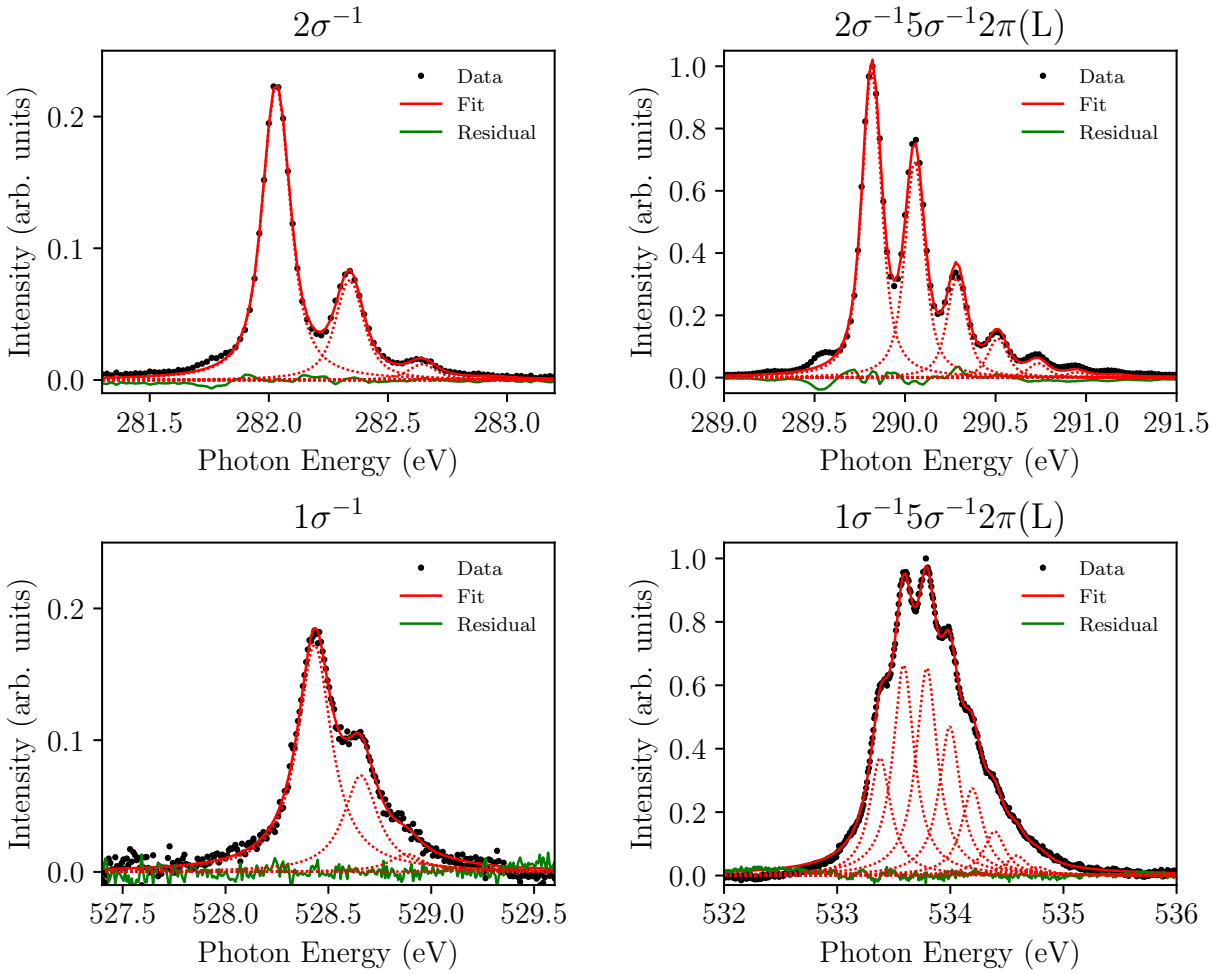

Figure S7: The transitions to the carbon K-edge $2\sigma^{-1}$ state (top left), carbon K-edge $2\sigma^{-1}5\sigma^{-1}2\pi$ state (top right) oxygen K-edge $1\sigma^{-1}$ state (bottom left) and oxygen K-edge $1\sigma^{-1}5\sigma^{-1}2\pi$(L) state (bottom right). The figure shows the experimental data (dots) and the curve fit for the Franck-Condon analysis (solid red line) with all contributions from the vibrationally ground state (dotted red line)

Assignment of NEXAFS spectrum

The complete assignment of all theoretical transitions for carbon K-edge, seen in Fig. S8, are presented in Tabs. S3 and S4. The assignment of the oxygen K-edge (Fig. S9) can be found in Tab. S5.

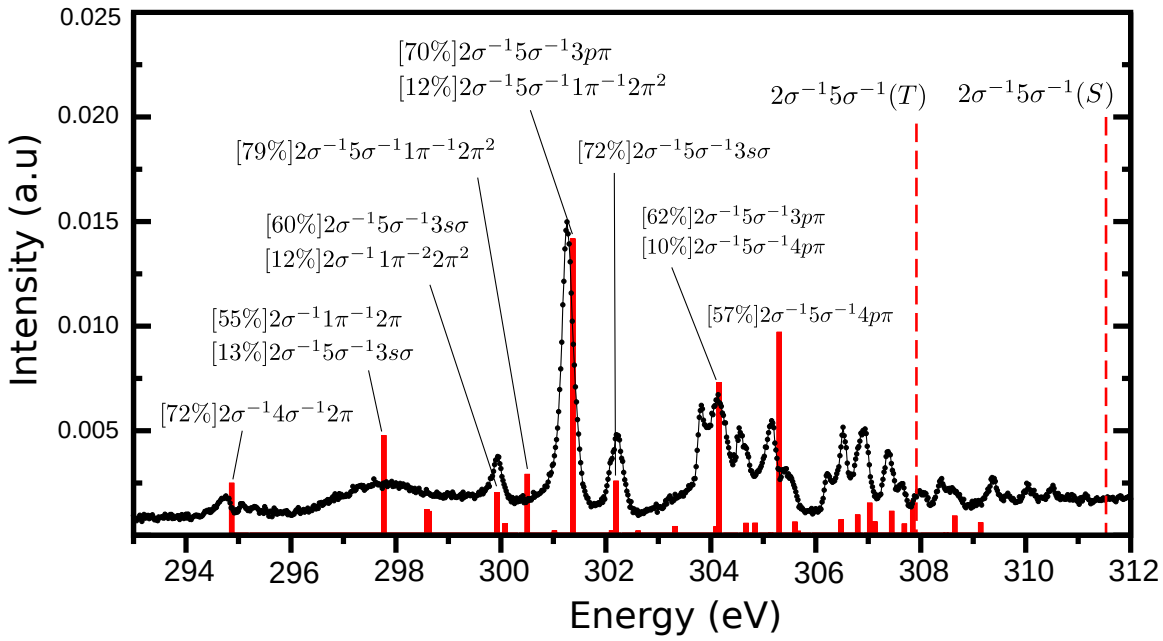

Figure S8: A zoom in the high energy region of CO^+ absorption spectrum at carbon K-edge. The theoretical spectrum (red bars) was shifted by −1.43 eV in order to match most experimental features (black curve).

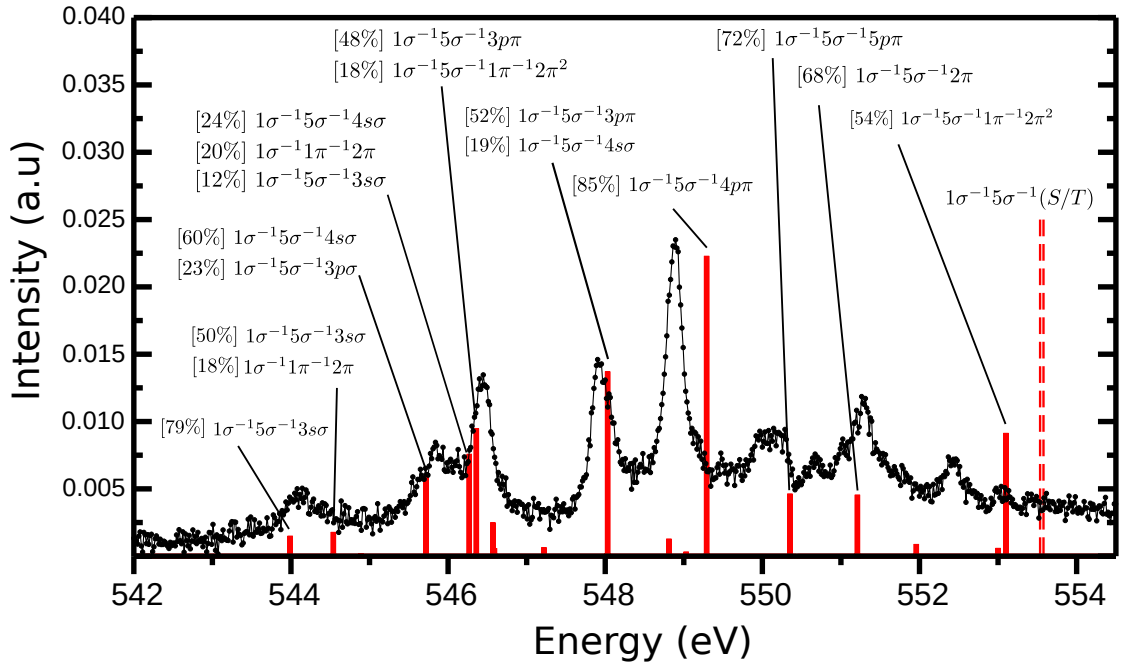

Figure S9: A zoom in the high energy region of CO^+ absorption spectrum at oxygen K-egde. The theoretical spectrum was shifted by −0.75 eV.

Table S3: Excitation energy, oscillator strength and assignment of all electronic states shown in the spectrum of carbon K-edge (Fig. S8). Shown in brackets are the weight of the CI coefficients of each configuration. Only configurations with a CI weight bigger than 10% are presented. The energies were shifted by −1.3 eV to match the experimental results in the high energy region.

State	Energy (eV)	Osc. Str. (a.u.)	[CI weight (%)] Assignment
1	281.35	2.48E-02	[86.8] $2\sigma^{-1}$
2	289.58	1.56E-01	[71.0] $2\sigma^{-1}5\sigma^{-1}2\pi$
3	290.03	6.58E-05	[90.5] $2\sigma^{-1}1\pi^{-1}2\pi$
4	290.31	3.53E-03	[73.3] $2\sigma^{-1}5\sigma^{-1}2\pi$
5	294.90	2.54E-03	[71.7] $2\sigma^{-1}4\sigma^{-1}2\pi$
6	295.23	8.49E-05	[70.9] $2\sigma^{-1}4\sigma^{-1}2\pi$ / [16.1] $2\sigma^{-1}5\sigma^{-1}1\pi^{-1}2\pi^2$
7	297.78	4.86E-03	[54.7] $2\sigma^{-1}1\pi^{-1}2\pi$ / [12.8] $2\sigma^{-1}5\sigma^{-1}3s\sigma$
8	298.60	1.26E-03	[79.2] $2\sigma^{-1}5\sigma^{-1}1\pi^{-1}2\pi^2$
9	298.64	1.17E-03	[87.9] $2\sigma^{-1}5\sigma^{-1}1\pi^{-1}2\pi^2$
10	299.92	2.09E-03	[60.0] $2\sigma^{-1}5\sigma^{-1}3s\sigma$ / [12.0] $2\sigma^{-1}1\pi^{-2}2\pi^2$
11	300.08	5.79E-04	[83.5] $2\sigma^{-1}5\sigma^{-1}1\pi^{-1}2\pi^2$
12	300.34	5.55E-05	[63.7] $2\sigma^{-1}1\pi^{-2}2\pi^2$ / [11.2] $2\sigma^{-1}1\pi^{-1}2\pi^1$
13	300.50	2.97E-03	[78.6] $2\sigma^{-1}5\sigma^{-1}1\pi^{-1}2\pi^2$
14	301.01	2.24E-04	[45.9] $2\sigma^{-1}5\sigma^{-2}2\pi^2$ / [16.6] $2\sigma^{-1}4\sigma^{-1}5\sigma^{-1}2\pi^2$
15	301.36	1.44E-02	[69.9] $2\sigma^{-1}5\sigma^{-1}3p\pi^1$ / [12.3] $2\sigma^{-1}5\sigma^{-1}1\pi^{-1}2\pi^2$
16	302.10	2.36E-04	[82.4] $2\sigma^{-1}5\sigma^{-2}2\pi^2$
17	302.16	2.21E-05	[94.0] $2\sigma^{-1}1\pi^{-2}2\pi^2$
18	302.18	2.64E-03	[72.1] $2\sigma^{-1}5\sigma^{-1}3s\sigma$
19	302.28	2.85E-05	[60.6] $2\sigma^{-1}1\pi^{-1}3s\sigma$ / [12.0] $2\sigma^{-1}5\sigma^{-1}1\pi^{-1}2\pi^2$
20	302.60	2.19E-04	[68.5] $2\sigma^{-1}1\pi^{-1}3s\sigma$ / [10.7] $2\sigma^{-1}1\pi^{-1}3p\sigma$
21	303.30	4.40E-04	[67.1] $2\sigma^{-1}1\pi^{-1}3p\sigma$
22	304.08	4.19E-04	[60.0] $2\sigma^{-1}5\sigma^{-1}4p\pi$ / [11.2] $2\sigma^{-1}1\pi^{-1}3p\sigma$
23	304.14	7.43E-03	[62.2] $2\sigma^{-1}5\sigma^{-1}3p\pi$ / [10.3] $2\sigma^{-1}5\sigma^{-1}4p\pi$

Table S4: Continuation of Tab.S3

State	Energy (eV)	Osc. Str. (a.u.)	[CI weight (%)] Assignment
24	304.21	6.78E-05	[56.4] $2\sigma^{-1}1\pi^{-1}3p\pi$ / [21.3] $2\sigma^{-1}1\pi^{-2}2\pi^2$
25	304.51	7.66E-05	[59.8] $2\sigma^{-1}4\sigma^{-1}1\pi^{-1}2\pi^2$
26	304.65	5.94E-04	[45.5] $2\sigma^{-1}1\pi^{-2}2\pi^2$ /[10.0] $2\sigma^{-1}1\pi^{-1}3p\pi$
27	304.79	5.96E-05	[38.6] $2\sigma^{-1}1\pi^{-1}4s\sigma$ / [39.7] $2\sigma^{-1}1\pi^{-1}3p\sigma$
28	304.82	5.98E-04	[54.5] $2\sigma^{-1}1\pi^{-1}3p\pi$ / [21.8] $2\sigma^{-1}1\pi^{-2}2\pi^2$
29	304.88	6.65E-05	[40.4] $2\sigma^{-1}1\pi^{-1}3p\sigma$ / [21.7] $2\sigma^{-1}1\pi^{-1}4s\sigma$ / [20.4] $2\sigma^{-1}4\sigma^{-1}1\pi^{-1}2\pi^2$
30	305.12	1.12E-04	[38.5] $2\sigma^{-1}1\pi^{-1}3p\pi$ / [30.2] $2\sigma^{-1}1\pi^{-2}2\pi^2$
31	305.18	6.67E-05	[66.6] $2\sigma^{-1}4\sigma^{-1}3s\sigma$
32	305.28	9.88E-03	[56.6] $2\sigma^{-1}5\sigma^{-1}5p\pi$
33	305.57	6.52E-04	[63.2] $2\sigma^{-1}4\sigma^{-1}5\sigma^{-1}2\pi^2$ / [12.5] $2\sigma^{-1}4\sigma^{-1}3s\sigma$
34	305.64	2.09E-04	[50.7] $2\sigma^{-1}4\sigma^{-1}1\pi^{-1}2\pi^2$
35	305.88	7.59E-05	[47.2] $2\sigma^{-1}4\sigma^{-1}3p\sigma$ / [16.1] $2\sigma^{-1}4\sigma^{-1}5\sigma^{-1}2\pi^2$
36	306.45	7.64E-04	[33.8] $2\sigma^{-1}4\sigma^{-1}1\pi^{-1}2\pi^2$ / [19.2] $2\sigma^{-1}5\sigma^{-1}1\pi^{-1}2\pi^2$
37	306.76	9.97E-03	[58.2] $2\sigma^{-1}4\sigma^{-1}3s\sigma$
38	306.87	2.45E-05	[27.5] $2\sigma^{-1}4\sigma^{-1}1\pi^{-1}2\pi^2$ / [25.2] $2\sigma^{-1}4\sigma^{-1}3p\pi$ / [16.3] $2\sigma^{-1}5\sigma^{-1}4p\pi$
39	306.99	1.57E-03	[51.1] $2\sigma^{-1}5\sigma^{-1}4p\pi$ / [20.0] $2\sigma^{-1}4\sigma^{-1}3p\pi$
40	307.09	6.67E-04	[34.4] $2\sigma^{-1}4\sigma^{-1}3p\pi$ / [34.5] $2\sigma^{-1}4\sigma^{-1}1\pi^{-1}2\pi^2$
41	307.41	1.18E-03	[35.5] $2\sigma^{-1}4\sigma^{-1}5\sigma^{-1}2\pi^2$ / [24.4] $2\sigma^{-1}1\pi^{-2}2\pi^2$
42	307.65	5.58E-04	[55.6] $2\sigma^{-1}5\sigma^{-1}5p\pi$
43	307.81	1.68E-03	[25.9] $2\sigma^{-1}5\sigma^{-1}1\pi^{-1}2\pi^2$ / [17.7] $2\sigma^{-1}5\sigma^{-1}5p\pi$
44	307.95	4.43E-05	[63.1] $2\sigma^{-1}4\sigma^{-1}2\pi$ / [11.1] $2\sigma^{-1}4\sigma^{-1}3p\sigma$
45	308.44	1.07E-04	[44.3] $2\sigma^{-1}5\sigma^{-1}5p\pi$ / [10.1] $2\sigma^{-1}4\sigma^{-1}3p\pi$
46	308.60	9.44E-04	[52.7] $2\sigma^{-1}4\sigma^{-1}3p\pi$ / [10.0] $2\sigma^{-1}5\sigma^{-1}5p\pi$
47	309.09	6.19E-04	[70.6] $2\sigma^{-1}4\sigma^{-1}3p\sigma$

Table S5: Excitation energy, oscillator strength and assignment of all electronic states shown in the spectrum of oxygen K-edge (Fig. S9).Shown in brackets are the weight of the CI coefficients of each configuration. Only configurations with a CI weight bigger than 10% are presented. The energies were shifted by −0.75 eV to match the experimental results in the high energy region.

State	Energy (eV)	Osc. Str. (a.u.)	[CI weight (%)] Assignment
1	528.10	5.63E-03	[89.8] $1\sigma^{-1}$
2	533.66	3.07E-02	[71.0] $1\sigma^{-1}5\sigma^{-1}2\pi$
3	537.04	9.07E-03	[69.7] $1\sigma^{-1}5\sigma^{-1}2\pi$
4	541.98	2.05E-05	[88.9] $1\sigma^{-1}1\pi^{-1}2\pi$
5	543.99	5.84E-04	[78.8] $1\sigma^{-1}5\sigma^{-1}3s\sigma$
6	544.54	6.95E-04	[50.2] $1\sigma^{-1}5\sigma^{-1}3s\sigma$ / [18.1] $1\sigma^{-1}1\pi^{-1}2\pi$
7	544.89	3.67E-05	[72.6] $1\sigma^{-1}4\sigma^{-1}2\pi$
8	545.72	2.28E-03	[59.7] $1\sigma^{-1}5\sigma^{-1}4s\sigma$ / [23.1] $1\sigma^{-1}5\sigma^{-1}3p\sigma$
9	546.27	2.93E-03	[24.5] $1\sigma^{-1}5\sigma^{-1}4s\sigma$ / [19.9] $1\sigma^{-1}1\pi^{-1}2\pi$ / [11.7] $1\sigma^{-1}5\sigma^{-1}3s\sigma$
10	546.36	1.83E-03	[48.3] $1\sigma^{-1}5\sigma^{-1}3p\pi$ / [18.2] $1\sigma^{-1}5\sigma^{-1}1\pi^{-1}2\pi^2$
11	546.57	4.83E-04	[40.5] $1\sigma^{-1}5\sigma^{-1}3p\pi$ / [15.5] $1\sigma^{-1}5\sigma^{-1}1\pi^{-1}2\pi^2$
12	546.59	1.15E-04	[64.7] $1\sigma^{-1}5\sigma^{-1}3p\pi$
13	547.22	1.26E-04	[62.8] $1\sigma^{-1}4\sigma^{-1}2\pi$
14	548.02	7.66E-05	[56.5] $1\sigma^{-1}5\sigma^{-2}2\pi^2$ / [22.6] $1\sigma^{-1}5\sigma^{-1}3p\sigma$
15	548.03	5.29E-03	[52.1] $1\sigma^{-1}5\sigma^{-1}3p\sigma$ / [18.9] $1\sigma^{-1}5\sigma^{-1}4s\sigma$
16	548.81	5.00E-04	[29.4] $1\sigma^{-1}5\sigma^{-1}3p\sigma$ / [25.6] $1\sigma^{-1}5\sigma^{-1}4s\sigma$
17	549.03	6.45E-05	[63.2] $1\sigma^{-1}5\sigma^{-1}1\pi^{-1}2\pi^2$
18	549.29	4.30E-03	[75.2] $1\sigma^{-1}5\sigma^{-1}4p\pi$
19	550.35	8.97E-04	[72.6] $1\sigma^{-1}5\sigma^{-1}5p\pi$
20	550.44	1.83E-05	[71.1] $1\sigma^{-1}5\sigma^{-1}5p\pi$
21	551.21	8.80E-04	[66.9] $1\sigma^{-1}5\sigma^{-1}2\pi$
22	551.96	1.75E-04	[63.7] $1\sigma^{-1}5\sigma^{-1}2\pi$
23	553.00	1.19E-04	[74.0] $1\sigma^{-1}1\pi^{-1}3p\sigma$
24	553.10	1.77E-03	[54.2] $1\sigma^{-1}5\sigma^{-1}1\pi^{-1}2\pi^2$
25	553.53	1.55E-05	[77.3] $1\sigma^{-1}1\pi^{-1}4p\sigma$

References

(1) Sorensen, L. K.; Lindh, R.; Lundberg, M. Gauge Origin Independence in Finite Basis Sets and Perturbation Theory. *Chem. Phys. Lett.* **2017**, *683*, 536 – 542.

(2) Lindblad, R.; Kjellsson, L.; Couto, R. C.; Timm, M.; Bülow, C.; Zamudio-Bayer, V.; Lundberg, M.; von Issendorff, B.; Lau, J. T.; Sorensen, S. L. et al. The X-ray Absorption Spectrum of the N_2^+ Molecular Ion. *Phys. Rev. Lett., accepted for publication*

(3) Matsumoto, M.; Ueda, K.; Kukk, E.; Yoshida, H.; Tanaka, T.; Kitajima, M.; Tanaka, H.; Tamenori, Y.; Kuramoto, K.; Ehara, M. et al. Vibrationally resolved C and O 1s photoelectron spectra of carbon monoxides. *Chem. Phys. Lett.* **2006**, *417*, 89–93.